Original Research Article

SAGE Open Medicine

Label-free quantitative proteomics reveals the mechanisms of Aurora kinase B in renal cell carcinoma

SAGE Open Medicine
Volume 12: 1–9
© The Author(s) 2024
Article reuse guidelines:
sagepub.com/journals-permissions
DOI: 10.1177/20503121241228474
journals.sagepub.com/home/smo
Sage

Yulong Li[1] and Yang Yang[2]

Abstract

Background: Renal cell carcinoma is the most common form of kidney cancer which is a global threat to human health, needing to explore effective therapeutic targets and treatment methods. Aurora kinase B acts as an important carcinogenic role in various kinds of tumors, while its mechanism in renal cell carcinoma is indistinct. Herein we explore the underlying mechanism of Aurora kinase B in renal cell carcinoma.

Methods and results: Label-free quantitative proteomics analysis was employed to analyze the differentially expressed proteins in 786-O cells which were treated with si-Aurora kinase B or si-ctrl. In the current study, 169 differentially expressed proteins were identified. The top 10 upregulated proteins were MX2, IFI44L, ISG20, DDX58, F3, IFI44, ECE1, PRIC285, NIT1, and IFIT2. The top 10 downregulated proteins were FKBP9, FSTL1, DDAH1, TGFB2, HMGN3, COIL, FAM65A, PTPN14, ARFGAP2, and EIF2C2. GO enrichment analysis showed that these differentially expressed proteins participated in biological processes, including defense response to virus, response to virus, and type I interferon signaling pathway. These differentially expressed proteins participated in cellular components, including focal adhesion, cell-substrate adherens junction, cell-substrate junction, and endoplasmic reticulum lumen. These differentially expressed proteins participated in molecule functions, including guanyl nucleotide binding, nucleotidase activity, double-stranded RNA binding, 2′-5′-oligoadenylate synthetase activity, and virus receptor activity. Kyoto Encyclopedia of Genes and Genomes pathway analysis showed that the significantly changed proteins including OAS3, OAS2, JAK1, TAP1, and RAC1 were involved in Epstein-Barr virus infection.

Conclusions: Taken together, our results demonstrate the possible mechanisms that Aurora kinase B may participate in renal cell carcinoma. These findings may provide insights into tumorigenesis and a theoretical basis for developing potential therapies of renal cell carcinoma.

Keywords
AURKB, label-free, proteomics, renal cell carcinoma, differentially expressed proteins

Date received: 28 October 2023; accepted: 5 January 2024

Introduction

Renal cell carcinoma (RCC) accounts for more than 90% of kidney cancers which belongs to one of the most common malignancies.[1] Clear cell renal cell carcinoma (ccRCC), papillary RCC (PRCC) and chromophobe RCC are the major subtypes of RCC. Localized RCC can be managed by surgery, whereas conventional chemotherapy has limited efficacy for metastatic RCC. Therefore, there is an ongoing need to explore novel therapeutic targets or more effective treatments of RCC. Further exploring the mechanism of RCC is helpful to the potential future for RCC research and therapy. There are various abnormal expression genes found in RCC, and some of them may act as oncogenes such as MUC12,[2] ELOVL5,[3] MBD2,[4] P4HA1,[5] and some may act as tumor suppressor genes such as SIRT5,[6] OSR1,[7] HOXA11,[8] CHD5[9] during the tumorigenesis and progression of cancer. Aurora kinase B (AURKB) is a member of the aurora kinase subfamily which acts as a vital function in mitosis. Previous studies have reported that AURKB was overexpressed in ccRCC samples and its expression was increasing with the

[1]Department of Gastroenterology, Shaanxi Provincial People's Hospital, Xi'an, China
[2]School of Public Health, Shaanxi University of Chinese Medicine, Xianyang, China

Corresponding author:
Yulong Li, Department of Gastroenterology, Shaanxi Provincial People's Hospital, No. 256, Youyi West Road, Xi'an 710068, China.
Email: liyulong0639@126.com

Creative Commons Non Commercial CC BY-NC: This article is distributed under the terms of the Creative Commons Attribution-NonCommercial 4.0 License (https://creativecommons.org/licenses/by-nc/4.0/) which permits non-commercial use, reproduction and distribution of the work without further permission provided the original work is attributed as specified on the SAGE and Open Access pages (https://us.sagepub.com/en-us/nam/open-access-at-sage).

development of ccRCC. [10] ALKBH5 could regulate AURKB expression through regulating the stability of AURKB mRNA, and finally accelerating the growth of RCC cell.[11] The expression of Aurora B was differentially upregulated in ccRCC and primary tumors in patients with lymph node involvement.[12] These studies showed that AURKB may have an important role in RCC, while the mechanism of AURKB in RCC still remains unclear. It is useful to detect the change of protein to better investigate the mechanism of AURKB in RCC for the vital role of protein in determining cell fates. We employed proteomic approach to detect the changes in protein abundance between si-AURKB and si-ctrl groups to explore the possible biological process and pathway through which AURKB may participate in RCC.

Methods

Cell culture

786-O cells were incubated in RPMI-1640 medium with 10% fetal bovine serum (Invitrogen) and cultured in a humidified atmosphere with 5% CO_2 at 37°C.

Quantitative real-time polymerase chain reaction (qRT-PCR)

The 786-O cells were seeded and after 24 h, cells were transfected with si-AURKB or control siRNA (si-ctrl). Si-AURKB sequences were as follows: 5′-UUU AGG UCC ACC UUG ACG AUG CGGC-3′ and 5′-GCC GCA UCG UCA AGG UGG ACC UAAA-3′.[13] Total RNA was obtained with Trizol reagent, cDNA was synthesized from total RNA by using PrimeScript RT Reagent Kit (Takara Bio). The AURKB mRNA expression was detected by SYBR Premix Ex Taq II Kit (Takara Bio) with GAPDH as control.

Protein sample preparation

786-O cells transfected with si-AURKB or si-ctrl, through sample lysis, calculation of protein concentration by BCA quantitative, acetone precipitation, re-suspend protein for tryptic digest, cleaning up of sodium deoxycholate, peptide desalting.

Nano-UPLC separation and LC–MS/MS analysis

2 μg polypeptides from each group were separated by a nano-UPLC and detected by the Q-Exactive mass spectrometry (Thermo Finnigan). Reversed-phase chromatographic column was used to analyze. The mobile phase A is H_2O with 0.1% formic acid, 2% acetonitrile, and the mobile phase B is H_2O with 80% acetonitrile, 0.1% formic acid. The sample was added into the chromatographic column by the automatic sampler, and then separated. A 120 min gradient at 300 nL/min flow rate. Gradient B: 8%–30% for 92 min, 30%–40% for 20 min, 40%–100% for 2 min, 100% for 2 min, 100%–2% for 2 min, 2% for 2 min. Data dependent acquisition was performed with positive mode and scanned parent ion *m*/*z* range of 350–1600. Twenty fragments were collected after each full scan. Orbitrap analyzer at a resolution of 70,000(@200 *m*/*z*) for MS1, and at a resolution of 17,500 for MS2; The automatic gain control target for MS1 was set to 3.0E + 6 with max IT 50 ms, and 5.0E + 4 with max IT 100 ms for MS2. The normalized collision energy is 27%, isolation window is 2 *m*/*z* and dynamic exclusion time was set at 30 s.

Bioinformatics analysis

Raw data is processed with MaxQuant. The protein database is from UNIPROT database. The quantitative type was label-free quantification (LFQ), trypsin was set as specific enzyme with a maximum of three missed-cleavage sites. oxidation [M] and acetyl [protein N-term] were set as variable modifications, Carbamidomethyl [C] was set as fixed modifiers (the maximum number of variable modifiers is 3). The false discovery rates of peptide and protein level was set to 0.01. Samples were standardized. The protein with ratio A/B > 1.5, $p \leqslant 0.05$, unique peptide $\geqslant 2$ was defined as those that significantly changed. Gene Ontology (GO), Kyoto Encyclopedia of Genes and Genomes (KEGG), and protein interaction analysis were performed to analyze the possible biological processes, molecular functions, cellular components, important metabolic and signaling pathways based on the differentially expressed proteins in two comparing groups.

Statistical analysis

Results are shown as means± SD. Difference analysis was assayed by Student's t- test. $p < 0.05$ was considered to indicate a statistically significant difference.

Results

Si-AURKB could suppress AURKB expression

QRT-PCR was employed to determine the mRNA expression of AURKB in 786-O cells which were transfected with si-AURKB or si-ctrl. The results showed AURKB expression in 786-O cells transfected with si-AURKB was significantly decreased comparing with si-ctrl transfected cells (Figure 1).

The cluster heat map

169 differentially expressed proteins were identified between si-AURKB transfected group and si-ctrl group by LFQ analysis. The heatmap grouped the similar data together by separately reorders the rows and columns. In order to determine the rationality and the accuracy of the differentially expressed proteins (DEPs), hierarchical clustering for each group of

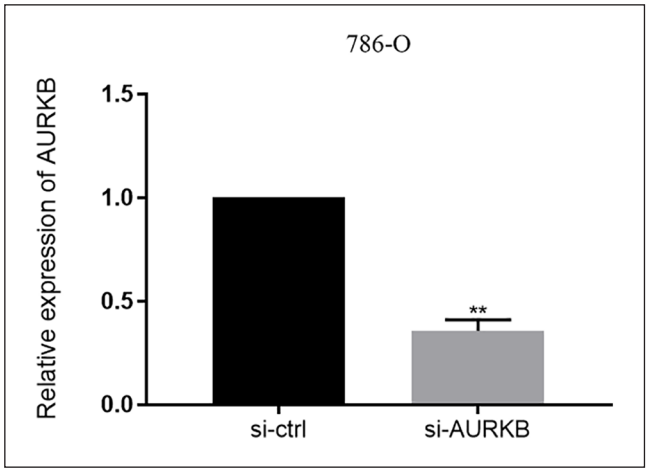

Figure 1. Si-AURKB inhibited the expression of AURKB in 786-O cells.
QRT-PCR was used to detect the expression of AURKB in 786-O cells transfected with si-AURKB or si-ctrl.
*p < 0.05.**p < 0.01.

samples was performed by using the selected proteins, as shown in Figure 2, the top color bar represents the grouping of samples; The bottom is the corresponding sample name; *Z*-core represents the relative expression level of protein by color. Detailed information of the top 10 upregulated proteins arranged by fold change (FC) is provided in Table 1. Information of the top 10 downregulated proteins arranged by FC is listed in Table 2.

Changes of significant proteins by volcano plot

Volcano plot could be used to recognize changes in large data sets. Volcano plot was increasingly common in genomics, proteomics, and metabolomics experiments. In this study, we used volcano plot to display the significantly changed proteins. The expression of 92 proteins significantly increased such as interferon-induced GTP-binding protein Mx2 (MX2), interferon-induced protein 44-like (IFI44L), interferon-stimulated gene 20 kDa protein (ISG20), antiviral innate immune response receptor RIG-I (RIGI, also known

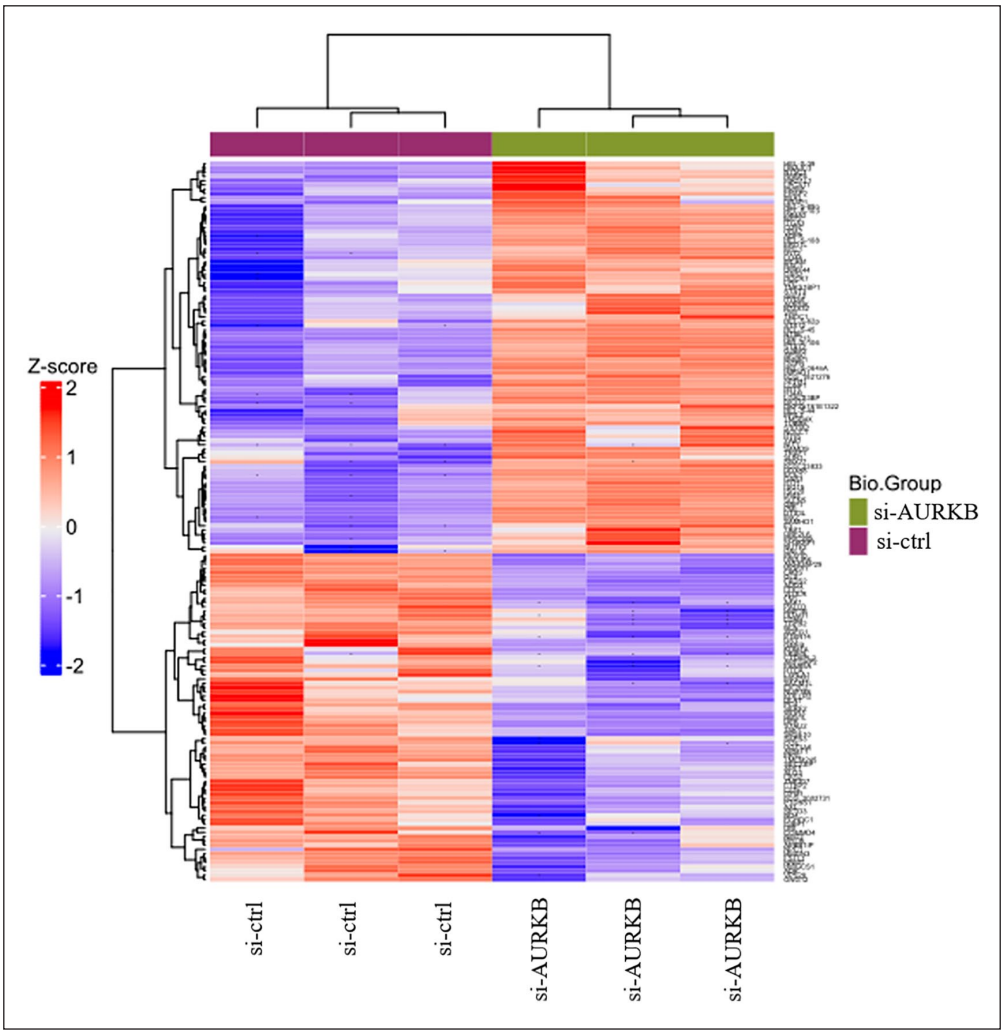

Figure 2. Heat map of the significant proteins in comparison of si-AURKB and psi-ctrl.

Table 1. Top 10 Significant proteins (upregulated).

Majority protein IDs	Gene names	Unique peptides	pv.si- AURKB–si-ctrl	fc.si- AURKB–si-ctrl
P20592	MX2	16	0.0001	62.0092
Q53G44	IFI44L	7	0.0014	18.9761
Q96AZ6	ISG20	2	0.0002	15.2621
O95786	DDX58	8	0.0012	13.2804
P13726	F3	5	0.0046	12.8959
Q8TCB0	IFI44	8	0.0005	12.5510
B4DKB2	ECE1	2	0.0005	9.2800
A7E2C9	PRIC285	11	0.0020	6.9312
Q86X76	NIT1	3	0.0135	4.95015
Q05DN2	IFIT2	3	0.0028	4.7480

Table 2. Top 10 Significant proteins (downregulated).

Majority protein IDs	Gene names	Unique peptides	pv si- AURKB–si-ctrl	fc.si-AURKB–si-ctrl
B7Z230	FKBP9	2	0.0293	0.1073
Q12841	FSTL1	9	0.0023	0.1796
B1AKK2	DDAH1	4	0.0039	0.2201
B2R7T2	TGFB2	2	0.0052	0.2274
Q15651	HMGN3	3	0.0008	0.2394
P38432	COIL	4	0.01862	0.2421
A0A0A0MTL6	FAM65A	2	0.0052	0.2483
B4DNZ0	PTPN14	2	0.0078	0.2783
B3KV00	ARFGAP2	2	0.0288	0.2802
A4FVC0	EIF2C2	4	0.0087	0.3012

as DDX58), tissue factor (F3), interferon-induced protein 44 (IFI44), endothelin converting enzyme 1 (ECE1), peroxisomal proliferator-activated receptor A interacting complex 285 (PRIC285), deaminated glutathione amidase (NIT1) and interferon-induced protein with tetratricopeptide repeats 2 (IFIT2), whereas that of 77 proteins such as high mobility group nucleosome-binding domain-containing protein 3 (HMGN3), transforming growth factor beta 2 (TGFB2), dimethylargininase (DDAH1), follistatin-related protein 1 (FSTL1) and FKBP prolyl isomerase 9 (FKBP9) were decreased as the volcano plot showed (Figure 3).

GO analysis

GO analysis was employed to investigate more insight on the biological significance of DEPs between si-AURKB group and si-ctrl group. GO enrichment analysis showed biological processes included defense response to virus, response to virus, type I interferon signaling pathway, cellular response to type I interferon, response to type I interferon, viral life cycle, viral genome replication, negative regulation of cytokine production, negative regulation of viral life cycle and negative regulation of viral genome replication. The cellular components included focal adhesion, cell-substrate adherens junction, cell-substrate junction, endoplasmic reticulum lumen, nuclear pore, actin filament, host, host cell, other organism and other organism cell. Top 10 molecule function were guanyl nucleotide binding, nucleotidase activity, double-stranded RNA binding, 2′-5′-oligoadenylate synthetase activity, virus receptor activity, hijacked molecular function, GTP binding, purine ribonucleoside binding, purine nucleoside binding and ribonucleoside binding (Figure 4(a)).

KEGG analysis

Different proteins coordinate with each other to exercise a series of biochemical reactions to perform biological functions. To examine which pathways and associated functions may be related with the expression of AURKB, KEGG enrichment analysis was performed and KEGG pathway mapping revealed Epstein-Barr virus (EBV) infection may be involved (Figure 4(b)). The significantly changed protein involved in Epstein-Barr virus infection including 2′-5′-oligoadenylate synthetase 3 (OAS3), 2′-5′-oligoadenylate synthetase 2 (OAS2), Janus kinase 1 (JAK1), transporter 1, ATP binding cassette subfamily B member (TAP1), Rac family small GTPase 1 (RAC1), and others.

Protein–protein interaction analysis

STRING[14] (https://cn.string-db.org/) could predict protein–protein interactions. Direct and indirect associations were

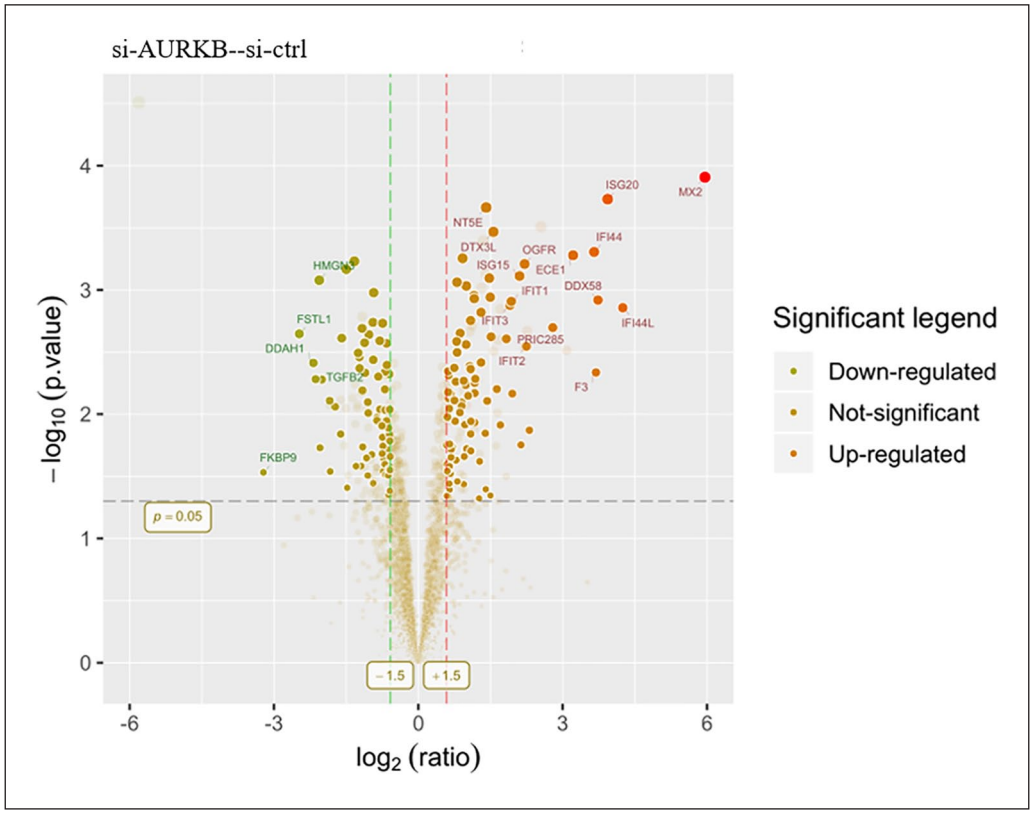

Figure 3. Different proteins shown by volcano plot. The red and green colors represent points-of-interest that show both large magnitude fold-changes and in *x* axis and high statistical significance in *y* axis.

included in the interactions. Edges represent protein–protein associations. The network of protein–protein interaction based on significance of DEPs between si-AURKB group and si-ctrl group is shown in Figure 4(c).

Discussion

AURKB plays the role of oncogene in many cancers such as gastric cancer,[15] colon cancer,[16] lung adenocarcinoma,[17] prostate cancer[18] and ccRCC.[19] Previous studies have reported that high AURKB expression indicated worse prognosis, and the expression of AURKB expression tended to rise with enhancing T stage and G grade of tumor.[20] AURKB is one of nine genes that related to poor survival of ccRCC analyzed by The Cancer Genome Atlas and Total Cancer Care data.[21] Bioinformatics analysis suggests that AURKB and KIF18B are closely related in ccRCC tissues, and when both of them are active they can accelerate the progression of ccRCC and indicate poor prognosis.[10] These studies suggested that AURKB may be a prospective target for the treatment of ccRCC patients.

Proteomics analysis was performed to explore the role of AURKB in RCC. One hundred sixty-nine significant proteins were identified between si-AURKB group and si-ctrl group. MX2, IFI44L, ISG20, DDX58, F3, IFI44, ECE1, PRIC285, NIT1, and IFIT2 are the top 10 upregulated significant proteins arranged by FC, and FKBP9, FSTL1, DDAH1, TGFB2, HMGN3, Coilin (COIL), RHO family interacting cell polarization regulator 1 (RIPOR1 also known as FAM65A), Tyrosine-protein phosphatase non-receptor type 14 (PTPN14), ADP ribosylation factor GTPase activating protein 2 (ARFGAP2) and argonaute RISC catalytic component 2 (AGO2, also known as EIF2C2) are the top 10 downregulated significant proteins. MX2, also known as MXB, the upregulation of MX2 is significantly related to the malignant phenotype of ccRCC and MX2 is a potential indicator for sunitinib resistance.[22] F3, also known as TF, postoperative serum levels of TF in patients with clear cell RCC were decreased and TF appears to be a potential marker of ccRCC.[23] IFI44 may be validated to identify high-risk patients who had worse prognosis than low-risk patients in ccRCC.[24] The expression of ECE-1 had no obvious difference between normal and tumor-affected tissue specimens from ccRCC patients, but the expression of ECE-1 was downregulated in PRCC tissues.[25] IFIT2 expression level was significantly lower in ccRCC tissues than in paracarcinoma tissues, and decreased expression of IFIT2 could predict poor survival in patients.[26] FSTL1 affects ccRCC through repressing the NF-κB and HIF-2α signaling pathways.[27] miR-200a was downregulated in renal cell carcinoma samples, and it suppressed RCC development via directly targeting TGFB2.[28] Bi-allelic

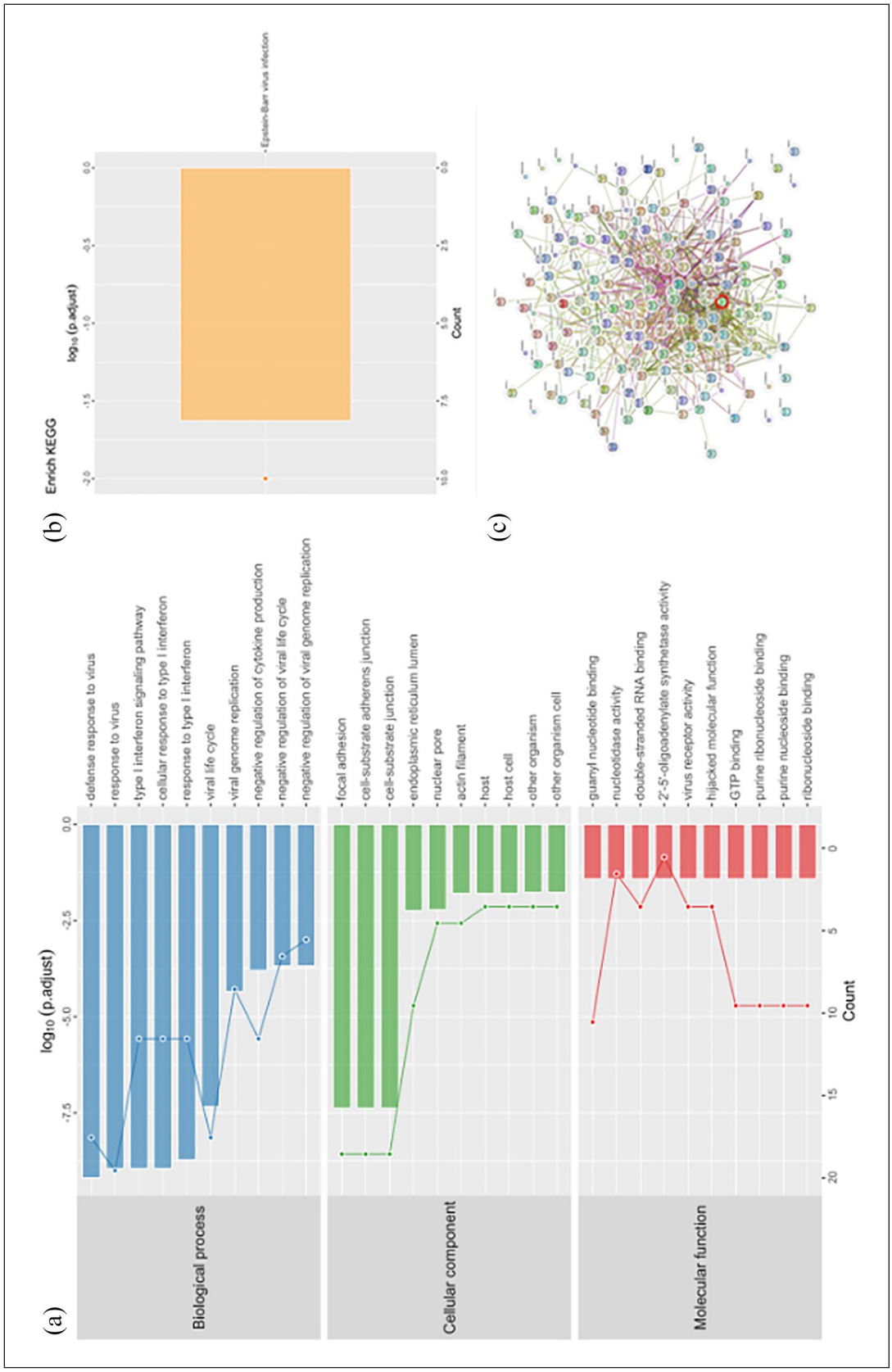

Figure 4. Bioinformatics results analysis. (a) Enriched GO items, the ontology covers biological process, cellular component and molecular function three domains. Top axis is log 10 (adjust *p*-value), bottom axis is the count of gene. (b) KEGG enrichment analysis of the alter proteins. KEGG enrichment reveals Epstein-Barr virus infection was involved. (c) Protein–protein network enrichment analysis was performed by search tool for the retrieval of interacting genes (STRING) to describe the significant proteins.

loss of PTPN14 was found in parts of mucinous tubular and spindle cell carcinoma.[29]

KEGG enrichment analysis was performed and revealed EBV infection may relate with the significant proteins. EBV as one of the most common viruses belongs to the Herpes family. EBV infects a large number of the population worldwide and relates to carcinogenesis with a common infection worldwide. EBV latent infection is lifelong and latently infected B cells transit the germinal center to transform resting memory cells according to germinal center model which is the model that explains EBV biology and the pathogenesis of lymphoma. Here, the virus remains stationary and occasionally reactivates to infect new B cells, finishing the infection cycle.[30] EBV lurks in lymphocytes for a long time and is separated from the cytoplasm through circular DNA, and it can integrate into the chromosome. A number of latent EBV expresses genes in the latent period and these genes may interact with oncogenes to cause host cell cycle disturbances, including G1/S transition, and suppression cell apoptosis, accelerating the advancement of EBV-related tumors.[31] Human EBNA1 binding protein 2 (hEBP2) binds to EBNA1, and hEBP2 is vital for the growth of human cells, inhibition hEBP2 could suppress the capacity of EBNA1 and EBV-based plasmids combine to mitotic chromosomes.[32] EBV is linked to various human cancers. EBV infection significantly increased the risk of breast carcinoma.[33] EBV infection decreases ferroptosis in nasopharyngeal carcinoma cells and EBV infection could activate p62-Keap1-NRF2 pathway and induce glutathione peroxidase 4 expression in nasopharyngeal carcinomacells, and GPX4 is related with chemoresistance in NPC cells infected with EB virus, and in multiple cancer patients with high expression of GPX4 is associated with poorer prognosis.[34] A high prevalence of EBV in prostate samples may indicate a possible association between EBV and the development of prostate cancers.[35] EBV affects the development of gastric cancer; EBV infection may induce the methylation of RASSF10 and promote cell growth in EBV-associated gastric cancer.[36] In EBV-associated hodgkin lymphoma patients, the EBV DNA load was related to prognosis; it may be a promising biomarker for EBV-positive Hodgkin lymphoma.[37] A subtype of intrahepatic cholangiocarcinoma was related to EBV.[38] There is increasing evidence that EBV infections may affect the risk and clinical course of malignancies; EBV infection is common in patients of RCC and it may add to the risk of high-grade RCC.[39] EBV-mediated RCC pathogenesis may have an association with the p65 NF-κB signaling pathway.[40] Previous studies showed that EBV was expressed in RCC and nephroblastoma, and the expression of EBV was related to RCC malignancy, suggesting that EBV may play an important role in RCC and nephroblastoma.[41] These reports suggested that EBV infection may represent a critical mechanism involved in the pathogenesis of RCC.

Although we have demonstrated the possible mechanisms of AURKB to the pathogenesis of RCC, this study had some limitations as well. Only one RCC cell line was used in this study; more RCC cell line and RCC tissues and their corresponding normal tissues should be used for the confirmation of the conclusion in the future. Moreover, we only performed the study in vitro; further validation of the conclusion is required through in vivo experiments.

Conclusion

By label-free quantitative proteomics, we found some differentially expressed proteins and pathway in RCC after knocking down AURKB. Collectively, this study shows the possible mechanisms of AURKB to the pathogenesis of RCC which may offer a theoretical basis for developing potential therapies of RCC.

Acknowledgements

Not applicable.

Author contributions

YL Li was responsible for the concept and design of the study; YL Li and Y Yang were involved with experimental and analytical aspects of the manuscript; YL Li and Y Yang undertook writing of the manuscript.

Declaration of conflicting interests

The author(s) declared no potential conflicts of interest with respect to the research, authorship, and/or publication of this article.

Funding

The author(s) disclosed receipt of the following financial support for the research, authorship, and/or publication of this article: This work was supported by Shaanxi Provincial People's Hospital science and technology talent support program (2021JY-64).

Ethics approval

Not applicable.

Informed consent

Not applicable.

Trial registration

Not applicable.

ORCID iD

Yulong Li https://orcid.org/0000-0002-4671-2471

References

1. Hsieh JJ, Purdue MP, Signoretti S, et al. Renal cell carcinoma. *Nat Rev Dis Primers* 2017; 3: 17009.

2. Gao SL, Yin R, Zhang LF, et al. The oncogenic role of MUC12 in RCC progression depends on c-Jun/TGF-beta signalling. *J Cell Mol Med* 2020; 24: 8789–8802.
3. Nitta S, Kandori S, Tanaka K, et al. ELOVL5-mediated fatty acid elongation promotes cellular proliferation and invasion in renal cell carcinoma. *Cancer Sci* 2022; 113: 2738–52.
4. Li L, Li N, Liu N, et al. MBD2 correlates with a poor prognosis and tumor progression in renal cell carcinoma. *Onco Targets Ther* 2020; 13: 10001–10012.
5. Li Y, Ge YZ, Qian Y, et al. The role of P4HA1 in multiple cancer types and its potential as a target in renal cell carcinoma. *Front Genet* 2022; 13: 848456.
6. Yihan L, Xiaojing W, Ao L, et al. SIRT5 functions as a tumor suppressor in renal cell carcinoma by reversing the Warburg effect. *J Transl Med* 2021; 19: 521.
7. Zhang Y, Yuan Y, Liang P, et al. OSR1 is a novel epigenetic silenced tumor suppressor regulating invasion and proliferation in renal cell carcinoma. *Oncotarget* 2017; 8: 30008–30018.
8. Wang L, Cui Y, Sheng J, et al. Epigenetic inactivation of HOXA11, a novel functional tumor suppressor for renal cell carcinoma, is associated with RCC TNM classification. *Oncotarget* 2017; 8: 21861–21870.
9. Du Z, Li L, Huang X, et al. The epigenetic modifier CHD5 functions as a novel tumor suppressor for renal cell carcinoma and is predominantly inactivated by promoter CpG methylation. *Oncotarget* 2016; 7: 21618–21630.
10. Liu Q, Zhang X, Tang H, et al. Bioinformatics analysis suggests the combined expression of AURKB and KIF18B being an important event in the development of clear cell renal cell carcinoma. *Pathol Oncol Res* 2020; 26: 1583–1594. DOI:10.1007/s12253-019-00740-y
11. Zhang X, Wang F, Wang Z, et al. ALKBH5 promotes the proliferation of renal cell carcinoma by regulating AURKB expression in an m(6)A-dependent manner. *Ann Transl Med* 2020; 8: 646.
12. Mathieu R, Patard JJ, Stock N, et al. [Study of the expression of Aurora kinases in renal cell carcinoma]. *Prog Urol* 2010; 20: 1200–1205.
13. Sakai S, Izumi H, Yoshiura Y, et al. In vitro evaluation of a combination treatment involving anticancer agents and an aurora kinase B inhibitor. *Oncol Lett* 2016; 12: 4263–4269.
14. Szklarczyk D, Gable AL, Nastou KC, et al. The STRING database in 2021: customizable protein-protein networks, and functional characterization of user-uploaded gene/measurement sets. *Nucl Acids Res* 2021; 49: D605–D612.
15. Nie M, Wang Y, Yu Z, et al. AURKB promotes gastric cancer progression via activation of CCND1 expression. *Aging (Albany NY)* 2020; 12: 1304–1321.
16. Peng S, Luo Y, Chen L, et al. lncRNA ELFN1-AS1 enhances the progression of colon cancer by targeting miR-4270 to upregulate AURKB. *Open Med (Wars)* 2022; 17: 1999–2012.
17. Gao X, Jiang A, Shen Y, et al. Expression and clinical significance of AURKB gene in lung adenocarcinoma: analysis based on the data-mining of bioinformatic database. *Medicine* 2021; 100: e26439.
18. Addepalli MK, Ray KB, Kumar B, et al. RNAi-mediated knockdown of AURKB and EGFR shows enhanced therapeutic efficacy in prostate tumor regression. *Gene Ther* 2010; 17: 352–359.
19. Wan B, Huang Y, Liu B, et al. AURKB: a promising biomarker in clear cell renal cell carcinoma. *PeerJ* 2019; 7: e7718.
20. Bao L, Zhao Y, Liu C, et al. The identification of key gene expression signature and biological pathways in metastatic renal cell carcinoma. *J Cancer* 2020; 11: 1712–1726.
21. Berglund A, Amankwah EK, Kim YC, et al. Influence of gene expression on survival of clear cell renal cell carcinoma. *Cancer Med* 2020; 9: 8662–8675.
22. Wei Y, Chen X, Ren X, et al. Identification of MX2 as a novel prognostic biomarker for sunitinib resistance in clear cell renal cell carcinoma. *Front Genet* 2021; 12: 680369.
23. Silva DD, Noronha JAP, Pinheiro da Costa BE, et al. Serum tissue factor as a biomarker for renal clear cell carcinoma. *Int Braz J Urol* 2018; 44: 38–44.
24. Wu X, Zhao Z, Khan A, et al. Identification of a novel signature and construction of a nomogram predicting overall survival in clear cell renal cell carcinoma. *Front Genet* 2020; 11: 1017.
25. Douglas ML, Richardson MM and Nicol DL. Endothelin axis expression is markedly different in the two main subtypes of renal cell carcinoma. *Cancer* 2004; 100: 2118–2124.
26. Xu B, Zhu YL, Fan JL, et al. Clinical significance of IFIT2 expression in human renal cancer tissues. *Transl Cancer Res* 2020; 9: 3214–3221.
27. Liu Y, Tan X, Liu W, et al. Follistatin-like protein 1 plays a tumor suppressor role in clear-cell renal cell carcinoma. *Chin J Cancer* 2018; 37: 2.
28. Lu R, Ji Z, Li X, et al. Tumor suppressive microRNA-200a inhibits renal cell carcinoma development by directly targeting TGFB2. *Tumour Biol* 2015; 36: 6691–6700.
29. Mehra R, Vats P, Cieslik M, et al. Biallelic alteration and dysregulation of the hippo pathway in mucinous tubular and spindle cell carcinoma of the kidney. *Cancer Discov* 2016; 6: 1258–1266.
30. Thorley-Lawson DA, Hawkins JB, Tracy SI, et al. The pathogenesis of Epstein-Barr virus persistent infection. *Curr Opin Virol* 2013; 3: 227–232.
31. Yin H, Qu J, Peng Q, et al. Molecular mechanisms of EBV-driven cell cycle progression and oncogenesis. *Med Microbiol Immunol* 2019; 208: 573–583.
32. Kapoor P, Lavoie BD and Frappier L. EBP2 plays a key role in Epstein-Barr virus mitotic segregation and is regulated by aurora family kinases. *Mol Cell Biol* 2005; 25: 4934–4945.
33. Jin Q, Su J, Yan D, et al. Epstein-Barr virus infection and increased sporadic breast carcinoma risk: a meta-analysis. *Med Princ Pract* 2020; 29: 195–200.
34. Yuan L, Li S, Chen Q, et al. EBV infection-induced GPX4 promotes chemoresistance and tumor progression in nasopharyngeal carcinoma. *Cell Death Differ* 2022; 29: 1513–1527.
35. Ahmed K, Sheikh A, Fatima S, et al. Detection and characterization of latency stage of EBV and histopathological

analysis of prostatic adenocarcinoma tissues. *Sci Rep* 2022; 12: 10399.
36. Gao Y, Fu Y, Wang J, et al. EBV as a high infection risk factor promotes RASSF10 methylation and induces cell proliferation in EBV-associated gastric cancer. *Biochem Biophys Res Commun* 2021; 547: 1–8.
37. Habeeb R, Al Hafar L and Monem F. EBV Plasma Epstein-Barr Virus (EBV) DNA as a biomarker for diagnosis of EBV-positive Hodgkin Lymphoma in Syria. *J Infect Dev Ctries* 2021; 15: 1917–1922.
38. Huang YH, Zhang CZ, Huang QS, et al. Clinicopathologic features, tumor immune microenvironment and genomic landscape of Epstein-Barr virus-associated intrahepatic cholangiocarcinoma. *J Hepatol* 2021; 74: 838–849.
39. Kryst P, Poletajew S, Wyczalkowska-Tomasik A, et al. Epstein-Barr Virus and human adenovirus viremia in renal tumors is associated with histological features of malignancy. *J Clin Med* 2020; 9: 3195.
40. Farhadi A, Namdari S, Chong PP, et al. Epstein-Barr virus infection is associated with the nuclear factor-kappa B p65 signaling pathway in renal cell carcinoma. *BMC Urol* 2022; 22: 17.
41. Shimakage M, Kawahara K, Harada S, et al. Expression of Epstein-Barr virus in renal cell carcinoma. *Oncol Rep* 2007; 18: 41–46.